

Performance of a Hybrid Electric Vehicle Using Reluctance Synchronous Machine Technology

Johan Malan and Maarten J. Kamper, *Member, IEEE*

Abstract—The performance of a parallel hybrid electric vehicle (HEV) with a small reluctance synchronous machine drive is presented. The machine is current-angle controlled for maximum torque per ampere or minimum kVA. This ensures that the machine is operated reasonably close to optimal efficiency for all loads. The calculated and measured performance results of the reluctance synchronous machine drive and the electric vehicle are given. The 28-kW-peak reluctance synchronous machine is used to drive the rear wheels of a small delivery vehicle through a differential. The conventional petrol-engine-propelled front drive is kept standard. Simulation and measured results show that, with the small reluctance synchronous machine drive generating a peak torque of 150 N·m, the 1480-kg vehicle accelerates from 0 to 60 km/h in 19 s. The maximum range of the HEV on a single battery charge is measured as 90 km at 60 km/h.

Index Terms—Hybrid electric vehicle, reluctance machine.

I. INTRODUCTION

THERE IS A widespread interest in electric vehicles (EVs) today. The reasons for this interest are, among other things, plus: 1) urban air pollution and global warming concerns; 2) an interest by power supply authorities to sell more product when loads on supply are not present [1]; and 3) the technical and economic advantages of using EVs. The last reason can be attributed to the developments in batteries, fuel cells, flywheels, low-emission engines, etc. However, the developments in power electronics and micro-processors together with new developments in analysis, design, and materials for high-power density electrical machines are equally important in making the EV technically and economically more viable today.

EVs can be classified into three categories. The first is those EVs that are powered from only one power source such as batteries or fuel cells. The second is those that are powered from an engine-generator system, generally called diesel-electric or engine-electric vehicles. Thirdly, there are those EVs that are powered from two power sources in a series or parallel mode, called hybrid electric vehicles (HEVs) [2], [3].

HEVs are currently receiving the greatest attention. With HEVs urban zero-emission driving can be combined with long-distance driving powered from the engine. A Delphi study concluded that HEVs would account for 5% of the

American car market in 2007 [4]. An example of a parallel HEV that is already in production is the Toyota Prius [5]. The engine-electric vehicle is also under consideration as an alternative to the internal combustion engine (ICE) vehicle (engine-gearbox-differential drive).

In all types of EVs one or more electric wheel drives are used, which is the very heart of the EV. Mainly four types of electric machines are used, or mentioned as a possibility for use, in EVs today [3], [6]–[8]. These are the dc-machine, induction machine (IM), permanent magnet machine (PM), and switched reluctance machine (SRM). Of these the induction and permanent magnet machines are used the most. Considerable attention is given in research and development to the permanent magnet machine due to the availability of high-energy-product magnets. West [3] compares the different electrical machine drives for EVs. His overall conclusion is that mainly the induction machine drive will be used for the next five years and then the permanent magnet machine drive beyond the five-year time span. The SRM drive is called by [3] the “dark horse” which may in future offer an intermediate capability between induction and permanent magnet machine drives. The outcome of Chang’s survey [6] is that the induction machine drive is preferred for EVs, with the permanent magnet brushless dc machine and SRM drives as alternative EV propulsion. Buckley [9] from Emerson Electric reports on a quieter SRM drive which could power EV into the next century.

From these studies, it is surprising that the reluctance synchronous machine (RSM) drive is not even mentioned as a possible alternative for EV propulsion. The paper will show that the RSM drive has almost all the advantages of the SRM drive and more. A brief comparison of the advantages and disadvantages of the IM, SRM, and RSM drives is given in the paper. The paper reports on the use and the performance of an RSM-propelled HEV. A brief background with recent research results of the RSM drive is given. The performance results of the RSM drive used for the HEV are given, the current control method used is described, and simulation and measured results of the HEVs performance are given.

II. BACKGROUND OF THE RSM DRIVE

The RSM has a standard three-phase stator winding and an unexcited rotor with magnetic asymmetry. No brushes, windings, or permanent magnets are used on the rotor. The RSM is generally not considered to be competitive in terms of power density and power factor. The reason for this perception lies in its performance in the past. It soon became clear that using the machine in an open-loop mode, i.e., with a fixed voltage and

Paper IPCSD 01–047, presented at the 2000 Industry Applications Society Annual Meeting, Rome, Italy, October 8–12, and approved for publication in the IEEE TRANSACTIONS ON INDUSTRY APPLICATIONS by the Industrial Drives Committee of the IEEE Industry Applications Society. Manuscript submitted for review May 1, 2000 and released for publication July 6, 2001.

The authors are with the Department of Electrical and Electronic Engineering, University of Stellenbosch, 7600 Stellenbosch, South Africa (e-mail: jmalan@ing.sun.ac.za; kamper@ing.sun.ac.za).

Publisher Item Identifier S 0093-9994(01)08310-4.

frequency supply, the power density and power factor of the machine are poor. With the machine in the closed-loop mode, i.e., with current and position feedback and using an inverter, the performance characteristics of the RSM change completely. This was shown and explained only recently. With closed-loop current vector control of the RSM, the spatial current placement in the machine with respect to the rotor can be controlled in such a way to maximize the torque to current ratio, or the efficiency or the power factor of the machine. From a design point of view, the performance of the RSM also benefits from the closed-loop current vector control scheme. A cage winding is no longer necessary and the machine can be designed to have the largest possible inductance difference and inductance ratio. There is in this case no problem of instability, as is the case with the open-loop control mode, if a too high inductance ratio is used.

Fratta and Vagati [10] for the first time applied a full vector control scheme to control the RSM. They show, together with Weh [11], that the RSM under closed-loop control has high-power density characteristics. A comparison between the RSM and the induction machine has been done by Fratta and Vagati [12], where they show that the RSM has a higher torque per volume capability than the induction machine counterpart in the 10–100-N·m torque range. Research on the RSM concentrated on the use of axially laminated rotors (i.e., the laminations are placed along the length of the rotor and then bent to form the salient poles) [13], [14], but Vagati [15] moves away from this type of rotor to the normal transverse laminated rotor with punched flux barriers. Recently Kamper [16] and Bomela [17] showed that the normal flux barrier rotor RSM has a good power density and efficiency relative to its induction machine counterpart.

III. RSM DRIVE FOR THE HEV

The RSM drive for the HEV consists of a flux barrier rotor RSM and a three-phase inverter and controller. A brief description of the drive components is given in the following sections.

A. Reluctance Synchronous Machine

The finite element optimum designed flux barrier rotor RSM used is shown in Fig. 1. The machine is air-cooled and has been built in a standard 5.5-kW line-started induction machine frame. At first, a standard shaft-mounted fan was used (instead of a separately mounted fan) to keep the costs low and the manufacturing and assembly process simple and standard. The use of a shaft-mounted fan implies that high torques at low speeds are only possible for relatively short times. However, it was found that the shaft-mounted fan is inefficient for driving in traffic due to frequent accelerations and decelerations. A separate dc fan was thus used to cool the machine, also internally. The machine with the dc cooling fan and drive shaft is shown in Fig. 2. The flux barrier rotor of Fig. 1 shows that its construction is simple with a standard laminated stack. The rotor is skewed by one stator slot pitch. The stator winding is also standard. The short time duration (2 min) peak torque of this RSM is 150 N·m up to a speed of 1800 r/min. This results in a peak output power of 28 kW. With the shaft-mounted fan, the rated low-speed power is 11.3 kW @ 1800 r/min. The rated high-speed power is 17



Fig. 1. Normal laminated flux barrier rotor RSM.



Fig. 2. The HEV's RSM with separate cooling fan and drive shaft.

kW @ 2700 r/min. This difference in the rated output power is due to the difference in cooling with the shaft-mounted fan at different speeds. The performance of the machine in the HEV, specifically in the low-speed region, is much better with the separate cooling fan and the rated power of the machine will also be higher. The measured results and performance of the machine are given in Section IV.

B. Inverter

The inverter used is shown in Fig. 3. The phases are switched in a four-quadrant unipolar switching mode. The four-quadrant topology is used to obtain a higher phase voltage from the available dc-bus. Using unipolar switching, the switching frequency at the terminals of the machine is twice the switching frequency of the IGBTs. This implies that the switching frequency can be lowered to have lower switching losses. The inverter can operate from a dc voltage of up to 400 V. For the power electronic switching bridges, two Fuji three-phase plus brake power blocks (7MBP200RA060) are used with an output peak current of 200 A. The power blocks consist of complete drive and protection circuitry for the IGBT inverter. The power blocks are mounted on two heat sinks which can be seen in Fig. 3. Forced fan cooling is used for the cooling of the heat sink. A low-inductance dc-bus layout is used between the dc link electrolytic and snubber capacitors. The dc and ac connectors can be seen on the rear side of the inverter.

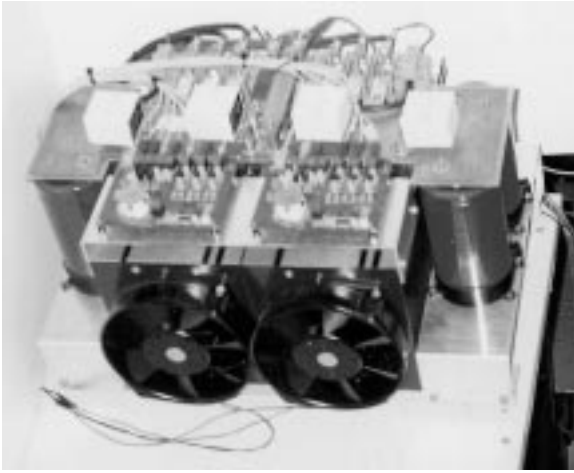


Fig. 3. Inverter for the RSM drive.

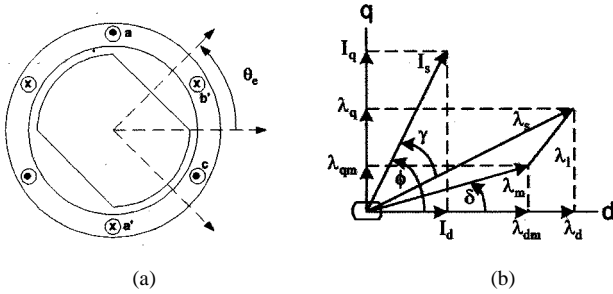


Fig. 4. (a) Cross section of the RSM and (b) space phasor diagram.

C. Controller

A constant current angle controller is used for the RSM below base speed, as explained by Kamper [18]. With this control the torque per rms current is always close to an optimum. To explain this briefly, consider the cross section and space phasor diagram of the RSM in Fig. 4. In Fig. 4(b), $I_s = I_d + jI_q$ and $\lambda_s = \lambda_d + j\lambda_q$ are the fundamental stator current and stator flux linkage space phasors, respectively. The stator flux linkage phasor λ_s originates from the current phasor I_s , and torque is produced when there is a phase shift between these phasors. The angle ϕ is the space phasor current angle which is the angle between the current space phasor and the d axis of the rotor.

The torque of the RSM in terms of dq -axis components for a p pole-pair machine can be expressed in the form

$$T = \frac{3}{2}p(L_d - L_q)I_dI_q \quad (1)$$

or

$$T = \frac{3}{2}p(L_d - L_q)I_s^2 \sin(2\phi). \quad (2)$$

The d - and q -axes inductances L_d and L_q are defined as $L_d = \lambda_d/I_d$ and $L_q = \lambda_q/I_q$. I_s in (2) is the amplitude of the current space phasor, or else the peak value of the phase currents. With constant current angle control below base speed, the phase current angle ϕ is kept constant at some value. The torque is thus varied by simply changing the phase current amplitude while keeping the position of the current space vector with respect to the rotor constant.

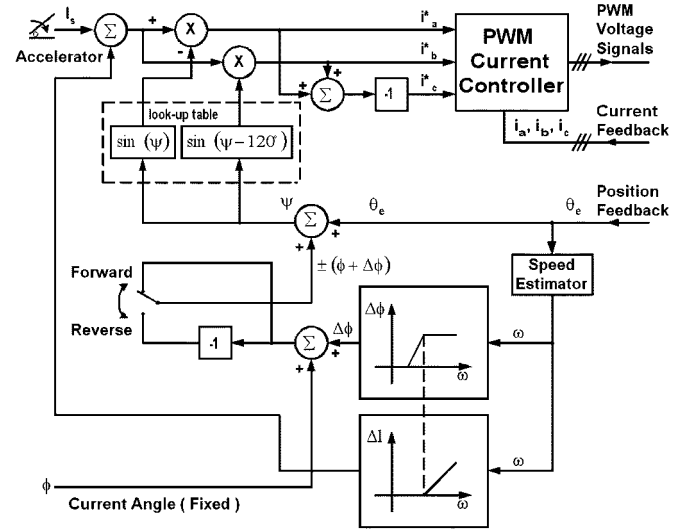


Fig. 5. Control block diagram of the RSM drive for the HEV.

This control is very much the same as the control of a dc series motor where the field flux varies with load. The advantages are that maximum torque per ampere is obtained independent of load and by this the RSM's efficiency is also reasonably close to optimal. The torque response is not as fast as with a fixed field current strategy, but with the large mechanical time constant of the EV the sacrifice in dynamic performance is insignificant. An optimum-efficiency control scheme for an RSM drive is also proposed by Matsuo [19], which is slightly more difficult to implement. At speeds above base speed, the current angle is increased (flux weakening mode) to a certain maximum value for the constant power speed range [18].

A very simple constant current angle controller is used for the HEV RSM drive as is shown in the block diagram of Fig. 5. The current reference signals are given by

$$\begin{aligned} i_a^* &= I_s \sin(\psi) \\ i_b^* &= I_s \sin(\psi - 120^\circ) \\ i_c^* &= I_s \sin(\psi + 120^\circ) \end{aligned} \quad (3)$$

where

$$\psi = \theta_e + (\phi + \Delta\phi) \text{ (forward mode)}$$

or

$$\psi = \theta_e - (\phi + \Delta\phi) \text{ (reverse mode)}. \quad (4)$$

In (4), θ_e is the electrical position of the rotor. With $\theta_e = 0$, the q axis of the rotor lies on the magnetic axis of phase a (Fig. 4). $\Delta\phi$ is an advanced angle used at high speeds for flux weakening (see Fig. 5).

The Park transformation is not used in the controller. To explain that the result is the same, assume, e.g., that $\theta_e = \phi = 0$. Then, according to (3), $i_a^* = 0$ and $i_b^* = -i_c^* = -0.866I_s$. Using then the Park transformation, $I_q = 0$ and $I_d = I_s$. Thus, only d -axis flux will be present. This is correct because with $\theta_e = 0$ in Fig. 4 and with only, but opposite, currents in phases b and c , flux will be generated only in the d -axis direction.

The current amplitude command, I_s , of Fig. 5 is controlled from the accelerator. The spatial current position in the machine is determined from the position sensor feedback and two sine

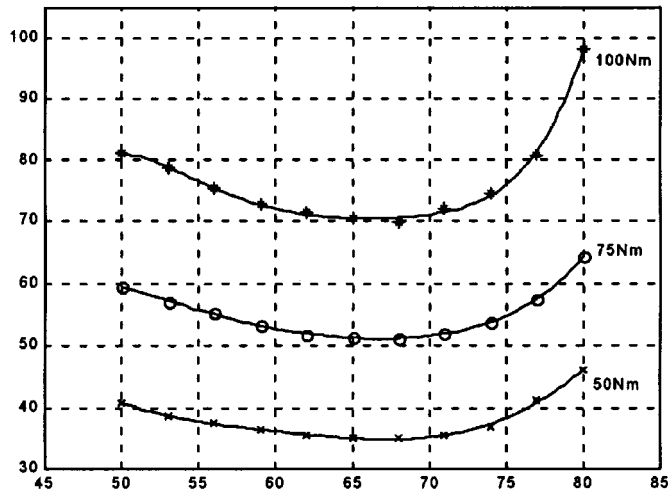


Fig. 6. Measured current versus current angle with torque as parameter.

functions (using lookup tables). The current angle is advanced at higher speeds as shown. The driver of the EV either selects forward or reverse, which simply changes the sign of the current angle to be added to the electrical position angle. Regenerative braking is done by switching from forward to reverse or vice versa when the brake pedal is used. The amount of regenerative braking can be adjusted by the driver with a potentiometer that overrides the signal from the acceleration pedal.

The controller can either be digital or partly digital-analog. For the developed system, a digital-analog control board is used. The sine functions are digitally generated from the digital input position signal ψ and are then output as analog signals through DACs. Two high-bandwidth analog multipliers (AD633) are used for the multiplication. For the closed-loop current control of the RSM, an analog current regulator with naturally sampled PWM (5 kHz) is used. Fiber-optic coupling is used between the current regulator and the inverter.

IV. MEASURED RESULTS OF RSM

In Fig. 6, the measured rms current versus the current angle ϕ of (2) is shown with the torque of the machine as a parameter. Hence, it is clear that maximum (or close to maximum) torque per ampere will always be obtained for all loads if the current angle is kept constant at some value, say 67° . Fig. 7 shows the measured efficiency versus current angle of the whole drive. It is clear that maximum (or close to maximum) efficiency for all loads will also be obtained with a constant current angle of 67° . This current angle is thus used in the block diagram of Fig. 5. In Fig. 8, the relation between torque and the rms current at the optimum current angle is shown. It is interesting that this relation is closely linear with a slight flattening at higher loads. This almost linear relation is in contrast with the quadratic relation of (2). However, the inductance difference of (2), $L_d - L_q$, is not a constant and varies due to saturation and cross magnetization [16]–[18]. The maximum torque of this RSM is 150 N·m, which can be delivered up to a speed of 1800 r/min. For speeds higher than the latter, the torque is reduced in an optimal control mode up to a maximum speed of 4500 r/min.

At the rated torque of 60 N·m and at a speed of 1800 r/min (11.3 kW), the temperature rise of the stator winding with the

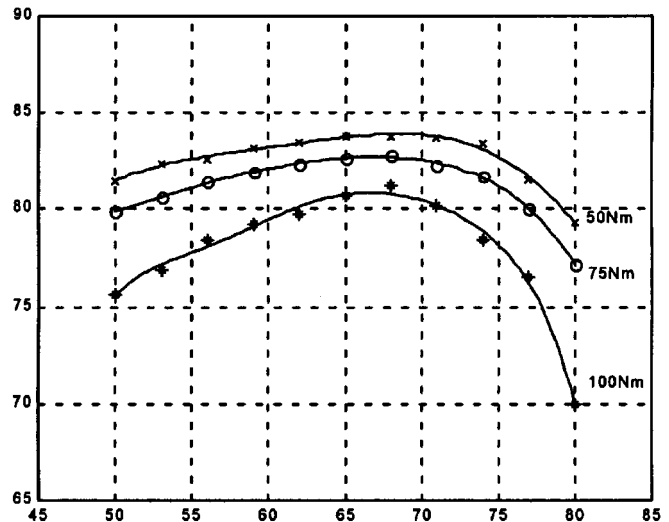


Fig. 7. Measured efficiency of the whole drive versus current angle with torque as a parameter at rated speed.

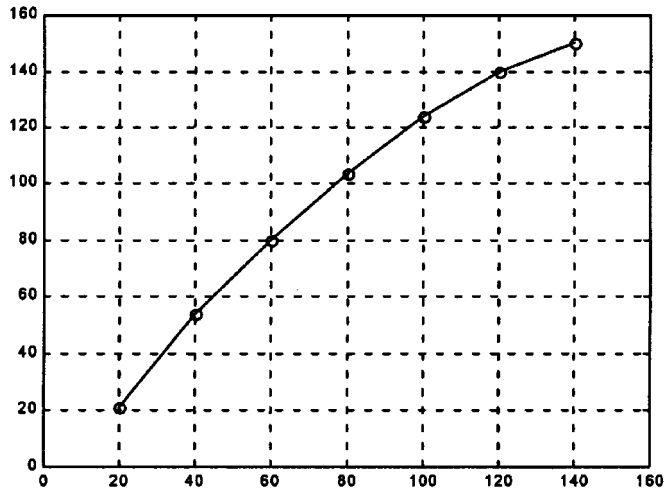


Fig. 8. Measured torque versus current of the RSM at optimum current angle.

shaft-mounted fan is measured as 106 K. At 2700 r/min and 60 N·m of torque (17 kW), the temperature rise is measured as 108 K. The latter is due to the better cooling at higher speeds with the shaft-mounted fan. The short time duration of the drive at 150 N·m is 2 min. With the use of the separate cooling fan in the HEV, the rated power of the machine will be higher.

V. HEV DESCRIPTION

The RSM drive was developed for a parallel HEV. This implies that the vehicle is propelled by an electric machine drive as well as a separate petrol-engine drive. A simple power diagram of the single-RSM-drive parallel HEV is shown in Fig. 9. The whole drive system is installed in a standard Mazda Rustler 1300, a small delivery vehicle (Fig. 10).

A single air-cooled RSM drive system is used which propels the rear wheels via a differential. The conventional petrol-engine propelled front drive is kept standard. Despite low energy density, lead-acid batteries are used due to cost and availability.

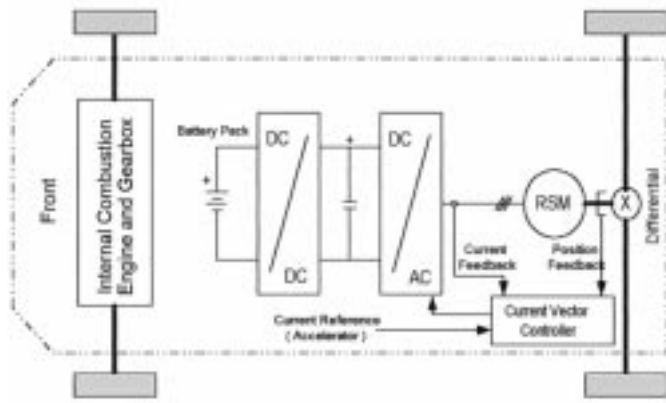


Fig. 9. Power diagram of parallel HEV.

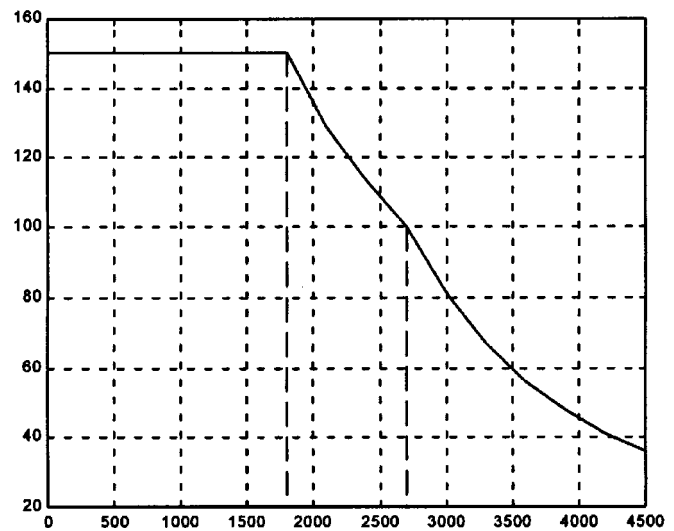


Fig. 11. Torque-speed curve of the RSM drive.



Fig. 10. Converted parallel HEV.

A pack of 22 × 12 V deep cycle batteries from Optima Batteries is used. It uses spiral technology that provides maximum power, fast and efficient recharge, and extremely low self-discharge. These batteries need zero maintenance, are completely sealed, and can be mounted in any position.

VI. PERFORMANCE OF THE HEV

To study the performance of the HEV, simulations of the acceleration of the original petrol vehicle and the converted HEV were performed. The software package used for the simulations was developed at the Department of Mechanical Engineering at the University of Stellenbosch. In the case of the HEV, the mass of the additional batteries, electric machine, and inverter (500 kg) is accounted for in the simulations.

The torque-speed characteristic of the single RSM drive is shown in Fig. 11. Four cases of acceleration are shown in Fig. 12. The measured acceleration results are given in Table I. In Fig. 12, it can be seen that the measured and simulated accelerations are very similar. It is clear that the 150-N·m RSM drive gives moderate to good performance compared to the petrol-propelled vehicle in the low-speed region. For speeds up to 100 km/h, the acceleration of the HEV with electric and petrol propulsion is the same as the standard vehicle. Thus, the electric propulsion compensates for the extra mass and no performance is lost. The maximum measured speed of the HEV with only electric propulsion is 60 km/h. With the dc-to-dc converter included (see Fig. 9), the dc-bus voltage will be

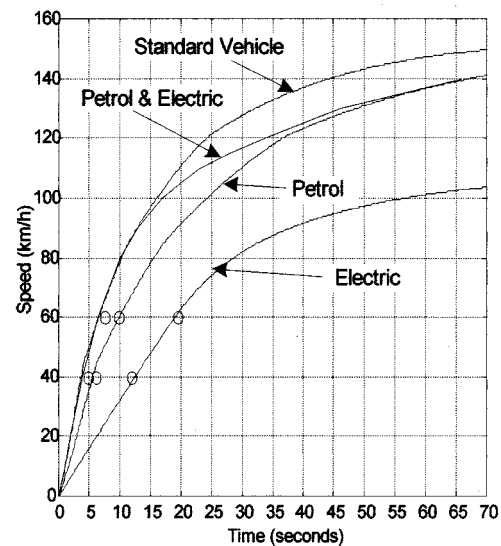


Fig. 12. Simulated and measured acceleration with different propulsions (O-measured).

TABLE I
MEASURED ACCELERATION TIME IN SECONDS

	Electric	Petrol	Petrol & Electric
0 - 40 km/h	11.9	6.2	4.9
0 - 60 km/h	19.5	9.8	7.6

high enough for the RSM to operate to its full potential in the high-speed region. This will make it possible for the HEV to reach a speed of 110 km/h with only the electric propulsion.

The HEV was also tested to determine the maximum range on a single battery charge. The test was done on a road with moderate uphill and downhill at a constant speed of 60 km/h. A range of 90 km was achieved. During this test, the maximum temperature rise of the RSM was only 35 K. The range on a flat road on a single battery charge is estimated to be about 120 km at 60 km/h.

VII. ADVANTAGES AND DISADVANTAGES

What are the advantages and disadvantages of the small RSM drive compared to the small IM and SRM drives? Compared to the IM drive, the advantages of the RSM lies in the torque density (28 N·m/L peak), torque per mass ratio (3.3 N·m/active-kg peak), efficiency (89%), cooling of the machine (there are no rotor losses), manufacturing costs (the rotor construction is simple), and a simple vector controller (there are no rotor parameters to be identified, as is clear from Fig. 5). The disadvantage of the RSM drive is the necessity of a position sensor, although position-sensorless control of the machine has been reported already, among others, in [20]. An advantage of the IM drive is the larger constant power speed range. The power factor of the IM is also better, which might result in a smaller kVA-rated inverter and a higher inverter efficiency.

Compared to the SRM drive, the RSM drive has all the advantages of the SRM drive except for the very wide speed range of the SRM. The speed of the flux barrier rotor RSM is to some extent limited by the mechanical strength of the rotor (this is more the case for the larger RSM). Also, the constant power speed range is not wide. Currently, the two important advantages of the RSM drive compared to the SRM drive are: 1) the drive is very much standard with a standard three-phase machine and standard inverter and 2) the RSM has a smooth torque down to zero speed. The relatively large torque pulsation and noise of the SRM drive are the main disadvantages of this drive.

VIII. CONCLUSION AND RECOMMENDATIONS

The small-to-medium power (say less than 50 kW) normal laminated flux barrier rotor RSM is shown to be well suited for EV applications. The good power density, power-to-weight ratio, efficiency, and effective cooling of the RSM are among its main advantages. As a standard manufactured drive with a simple rotor construction, the cost of the medium-power flux barrier rotor RSM drive will be low, despite the possible higher kVA-rating inverter required. The flux barrier rotor RSM drive must therefore be added to the list of possible drives for the EV.

The 150-N·m RSM drive with 22 lead-acid batteries (420 kg) gives moderate to good performance compared to the petrol-propelled vehicle. For speeds up to 100 km/h, the acceleration of the HEV with petrol and electric propulsion is the same as the standard vehicle and no performance is lost. A range of 90 km was achieved on a single battery charge at 60 km/h.

With a new machine design, using the finite element method and including thermal design aspects, the performance of the RSM can be improved further. Also, with the dc-to-dc converter of Fig. 9, a higher dc-bus voltage can be obtained to operate the RSM drive and the HEV over its full speed range.

REFERENCES

- [1] C. Snyman, "South Africa is poised to welcome the age of the EV," in *Proc. Electric & Hybrid Vehicle Technology '95 Conf.*, 1995, pp. 297–299.
- [2] V. Wouk, "Hybrids: Then and now," *IEEE Spectrum*, vol. 32, pp. 16–21, July 1995.
- [3] J. G. W. West, "DC, induction, reluctance and PM motors for electric vehicles," *Power Eng. J.*, pp. 77–88, Apr. 1994.
- [4] M. J. Riezenman and W. D. Jones, "EV watch," *IEEE Spectrum*, vol. 35, p. 16, Dec. 1998.

- [5] D. Hermance and S. Sasaki, "Hybrid electric vehicles take to the streets," *IEEE Spectrum*, vol. 35, pp. 48–52, Nov. 1998.
- [6] L. Chang, "Comparison of AC drives for electric vehicles—A report on experts' opinion survey," *IEEE Aerosp. Electron. Syst. Mag.*, vol. 9, pp. 7–11, Aug. 1994.
- [7] D. J. Paterson, "High efficiency permanent magnet drive systems for electric vehicles," in *Proc. IEEE IECON'97*, vol. 2, New Orleans, LA, Nov. 1997, pp. 391–396.
- [8] C. C. Chan, "Present status and future trends of electric vehicles," in *Proc. IEE 2nd Int. Conf. Advances in Power System Control, Operation and Management*, Hong Kong, Dec. 1993, pp. 456–467.
- [9] G. W. Buckley, "Making the switch," in *Proc. Electric & Hybrid Vehicle Technology '95 Conf.*, 1995, pp. 162–165.
- [10] A. Fratta, A. Vagati, and F. Villata, "A reluctance motor drive for high dynamic performance applications," in *Conf. Rec. IEEE-IAS Annu. Meeting*, 1987, pp. 295–302.
- [11] H. Weh, "Zur weiterentwicklung wechsellrichtergespeister reluctance maschinen für hohe leistungsdichten und große leistungen," *ETZ Arch.*, vol. 6, no. 4, pp. 135–141, 1984.
- [12] A. Fratta and A. Vagati, "Synchronous reluctance vs induction motor: A comparison," in *Proc. Intelligent Motion Conf.*, Nuremberg, Germany, Apr. 1992, pp. 179–186.
- [13] I. Boldea, Z. X. Fu, and S. A. Nasar, "Performance evaluation of axially-laminated anisotropic (ALA) rotor reluctance synchronous motors," in *Conf. Rec. IEEE-IAS Annu. Meeting*, Houston, TX, Oct. 1992, pp. 212–218.
- [14] T. Matsuo and T. A. Lipo, "Rotor design optimization of synchronous reluctance machine," *IEEE Trans. Energy Conversion*, vol. 9, pp. 359–365, June 1994.
- [15] A. Vagati, G. Franceschini, I. Marongiu, and G. P. Troglia, "Design criteria of high performance synchronous reluctance motors," in *Conf. Rec. IEEE-IAS Annu. Meeting*, Sept. 1992, pp. 66–73.
- [16] M. J. Kamper, F. S. van der Merwe, and S. Williamson, "Direct finite element design optimization of the cageless reluctance synchronous machine," *IEEE Trans. Energy Conversion*, vol. 11, pp. 547–553, Mar. 1996.
- [17] X. B. Bomela, S. K. Jackson, and M. J. Kamper, "Performance of small and medium power flux barrier rotor reluctance synchronous machine drives," in *Proc. ICEM*, vol. 1, Sept. 1998, pp. 95–99.
- [18] M. J. Kamper and A. T. Mackay, "Optimum control of the reluctance synchronous machine with a cageless flux barrier rotor," *Trans. S. Afr. Inst. Elect. Eng.*, vol. 86, no. 2, pp. 49–55, June 1995.
- [19] T. Matsuo, A. El-Antably, and T. A. Lipo, "A new control strategy for optimum-efficiency operation of a synchronous reluctance motor," *IEEE Trans. Ind. Applicat.*, vol. 33, pp. 1146–1153, Sept./Oct. 1997.
- [20] A. Consoli, F. Russo, and G. Scarcella, "Low- and zero-speed sensorless control of synchronous reluctance motors," *IEEE Trans. Ind. Applicat.*, vol. 35, pp. 1050–1057, Sept./Oct. 1999.



Johan Malan was born in South Africa in 1974. He received the B.Eng. degree in 1997 from the University of Stellenbosch, Stellenbosch, South Africa, where he is currently working toward the M.Eng. degree.

His main interests are electrical machine control, power electronics, and variable-speed drives. He is also currently with MLT-drives, South Africa.



Maarten J. Kamper (M'96) was born in South Africa in 1959. He received the B.Eng., M.Eng., and Ph.D. degrees from the University of Stellenbosch, Stellenbosch, South Africa, in 1983, 1987, and 1996, respectively.

He joined the lecturing staff of the University of Stellenbosch in 1989 and is currently an Associate Professor of electrical machines and drives. His main interest is electrical machine design using finite-element analysis and optimization algorithms. He is currently focusing on reluctance, axial flux permanent-magnet, and transverse flux machines for traction/wheel drive and generator applications.

Prof. Kamper is a Registered Professional Engineer in South Africa.